Hindawi Publishing Corporation
International Journal of Optics
Volume 2013, Article ID 876474, 6 pages
http://dx.doi.org/10.1155/2013/876474

Research Article

Ultrabroadband, Midinfrared Supercontinuum Generation in Dispersion Engineered As_2Se_3-Based Chalcogenide Photonic Crystal Fibers

Rim Cherif and Mourad Zghal

Gres'Com Laboratory, Engineering School of Communication of Tunis (Sup'Com), University of Carthage, Ghazala Technopark, 2083 Ariana, Tunisia

Correspondence should be addressed to Rim Cherif; rim.cherif@supcom.rnu.tn

Received 23 February 2013; Accepted 22 October 2013

Academic Editor: Marek Samoc

Small core As_2Se_3-based photonic crystal fibers (PCFs) are accurately characterized for compact, high power, ultrabroadband, and coherent supercontinuum generation within few millimeters fiber length. Bandwidths of ~5.3 μm, 5 μm, and 3.2 μm were calculated for hole-to-hole spacings $\Lambda = 3.5\,\mu$m, 4.5 μm, and 5.5 μm, respectively. The spectral broadening in the chalcogenide PCF is mainly caused by self-phase modulation and Raman-induced soliton self-frequency shift. The results show that small core As_2Se_3 PCFs are a promising candidate for mid-IR SCG up to ~8 μm.

1. Introduction

Supercontinuum generation (SCG) brings into play the nonlinear effects of Kerr and Raman, in combination with dispersion profiles of optical fibers, to broaden the bandwidth of an optical signal [1, 2]. Silica fibers have been the main source of SCG to date [3]. However, the longest wavelength that can be generated in silica fibers is below 2.5 μm due to material losses. Thus, SCG beyond this wavelength requires fibers with longer infrared (IR) transmission windows, along with an appropriate choice of dispersion and nonlinearity [4, 5]. Midinfrared photonics is seeing an increasing number of applications across a variety of disciplines such as astronomy and spectroscopy [6]. Price et al. [7] have shown theoretically that it is possible to generate a mid-IR supercontinuum from 2 to 5 μm using a bismuth-glass photonic crystal fiber (PCF). Domachuk et al. [8] have experimentally generated a mid-IR supercontinuum with a spectral range of 0.8 to 4.9 μm using a tellurite PCF with the same structure. Shaw et al. have reported experimental work that demonstrates supercontinuum generation from 2.1 to 3.2 μm in an As_2Se_3-based chalcogenide PCF with one ring of air holes in a hexagonal structure [9]. Hu et al. presented results of optimization of the SC bandwidth in an As_2Se_3-based PCF [10]. Compared to tellurite glass, chalcogenide glasses have shown their greater interest because of their larger refractive index and higher nonlinear index, leading to a greater modal confinement and a higher nonlinearity [11, 12]. In a recent paper, we studied SCG in one specific As_2Se_3-based PCF structure having a hole diameter $d = 1.26\,\mu$m and a hole-to-hole spacing $\Lambda = 1.77\,\mu$m [13]. However, such a study remains incomplete because it does not answer the question how a specific set of values for various dispersion coefficients can affect the generated bandwidth of the SC.

In this paper we identify specific dispersion profiles and correlate them with generated SC bandwidth. Our numerical simulations indicate that designed dispersion profile of the PCF is an excellent predictor of the generated bandwidth of the supercontinuum produced at the fiber output. We study a variety of As_2Se_3 dispersion profiles of PCF and their impact on SC generation in detail. This is the first time to our knowledge that SC generation is investigated in As_2Se_3-based PCF with Λ ranging from 3.5 to 5.5 μm. A full modal analysis of the optical properties of the designed PCFs is presented in terms of chromatic dispersion, effective area, and nonlinear coefficient. We find broad-bandwidth,

mid-IR, flat SC generation using few millimeters length of highly nonlinear As_2Se_3-based PCF. We find that Raman-induced soliton self-frequency shift effect is responsible for the generation of more than three octaves SC in As_2Se_3-based PCF with $d/\Lambda = 0.4$ and pitch varying from 3.5 μm to 5.5 μm.

2. Characterization of Optical Properties and Nonlinear Response of Different As_2Se_3-Based PCF Structures

The solid-core PCFs used in the numerical analysis reported in this paper have a hexagonal geometry. In our study, we optimize the PCF geometry over the single parameter of the air-hole pitch Λ and we choose different designed PCFs with $\Lambda = 3.5\,\mu$m, $4.5\,\mu$m, $5.5\,\mu$m, and $d/\Lambda = 0.4$. This value of the d/Λ ratio has been chosen in order to guarantee the single mode operation of the PCF and minimize the leakage loss. It is advantageous to maximize d/Λ in order to decrease the effective index of the cladding material and consequently enhance the nonlinearity and the modal confinement.

The first step in calculating the growth of the SCG is the determination of the chromatic dispersion and the nonlinear response which are needed to solve the generalized nonlinear Schrodinger equation (GNLS) [14]. Since our objective here is SC analysis mainly in the IR region, the chalcogenide PCF is a preferred choice leading to the investigation of the corresponding generated SC in As_2Se_3 glass which has very high nonlinear coefficient. In fact, chalcogenide glass exhibits wide bulk transparency (2–14 μm), high refractive index, and large nonlinearity in the mid-IR spectrum [11]. Figure 1 shows the selection of the calculated dispersion profiles of the designed PCF. The dispersion coefficient including both waveguide and material dispersion is proportional to the second derivative of effective index of guided mode with respect to wavelength and is given by [15]

$$D_c = -\frac{\lambda}{c}\frac{d^2 n_{\text{eff}}}{d\lambda^2}, \tag{1}$$

where "n_{eff}" is effective index of a guided mode calculated by means of the finite element method and c is the velocity of light in vacuum. To evaluate the wavelength dependant dispersion from the second derivative of the effective-mode index, Sellmeier equation is applied: $n(\lambda) = \sqrt{A + (B\lambda^2/(\lambda^2 - D)) + C\lambda^2}$: where $A = -4.5102$, $B = 12.0582$, $C = 0.0018\,\mu\text{m}^{-2}$, and $D = 0.0878\,\mu\text{m}^2$ [13].

We clearly see from Figure 1 that the dispersion curves exhibit one or more zero dispersion wavelengths (ZDW) with increasing separation for larger structures. We also observe a redshift of the first ZDW towards the infrared region when increasing Λ, for a fixed d/Λ ratio. When increasing the hole-to-hole spacing, the anomalous dispersion region broadens and shifts towards longer wavelengths. The ability of PCF to tailor the dispersion profiles through several degrees of structural freedom (Λ, d) opens up the possibility of seeding with large wavelengths (4.5–8 μm) in the mid-IR for optimum phase matching of nonlinear optical processes leading to the SC generation, as discussed in more detail in Section 3.

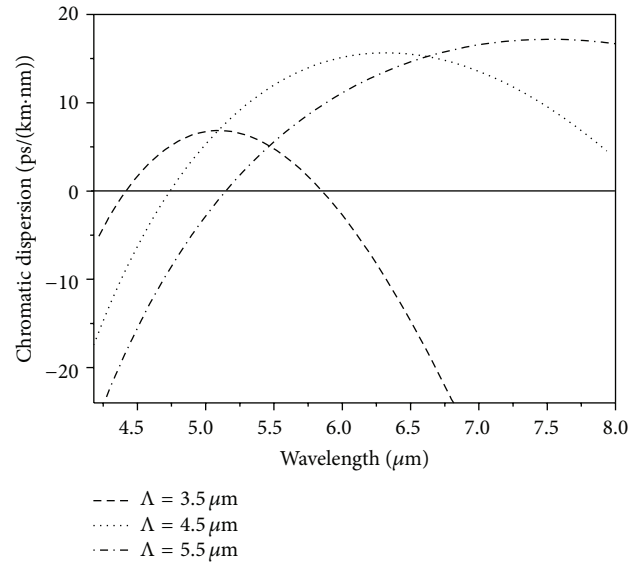

Figure 1: Chromatic dispersion for hexagonal PCFs with pitches of 3.5 μm (dashed), 4.5 μm (dotted), and 5.5 μm (dashed dotted).

Table 1: Table summarizing the optogeometrical properties of the three As_2Se_3-based PCF under investigation.

	d (μm)	Λ (μm)	ZDW (μm)	γ ($W^{-1}km^{-1}$)	λ_p (nm)
PCF 1	1.4	3.5	4.4 & 5.8	2409	4.6
PCF 2	1.8	4.5	4.7	1317	4.8
PCF 3	2.2	5.5	5.2	791	5.3

We also calculate the effective area (A_{eff}) and the nonlinear coefficient (γ) of the studied PCF. The Ultra parameters of the three PCF under investigation are summarized in Table 1. The effective area and the nonlinear coefficients are calculated at the chosen optimized pump wavelength (λ_p) of each structure. In our simulations of the SCG, we have chosen to pump close to the ZDW in the anomalous dispersion regime to maximize the generated bandwidths.

The studied As_2Se_3-based chalcogenide PCFs are designed to have specific dispersion profiles and high nonlinear coefficients γ. Following the full modal calculations of the As_2Se_3-based PCF properties, we need to determine the Raman contribution $h_R(t)$ of the As_2Se_3 chalcogenide material. To this end, we used the measured Raman gain spectrum of an As_2Se_3-based fiber reported in [6]. The temporal Raman response $h_R(t)$ is related to the Raman gain spectrum by $g_R(f) = (2\omega_p/c)n_2 f_R\,\text{Im}[H_R(f)]$, where ω_p is the pump frequency and $\text{Im}[H_R(f)]$ is the imaginary part of the Fourier transform of $h_R(t)$. The determination of the delayed Raman response $h_R(t)$ which is expressed through the Green's function of the damped harmonic oscillator: $h_R(t) = ((\tau_1^2 + \tau_2^2)/\tau_1\tau_2^2)\exp(-t/\tau_2)\sin(t/\tau_1)$ is fulfilled by taking the inverse Fourier transformation of the Raman gain and fitting it with a lorentzian profile (Figure 2). Thus, the calculated parameters $\tau_1 = (1/2\pi f_R) = 23$ fs and $\tau_2 = (1/\sqrt{2}\pi\Delta f) = 164.5$ fs were here found to yield

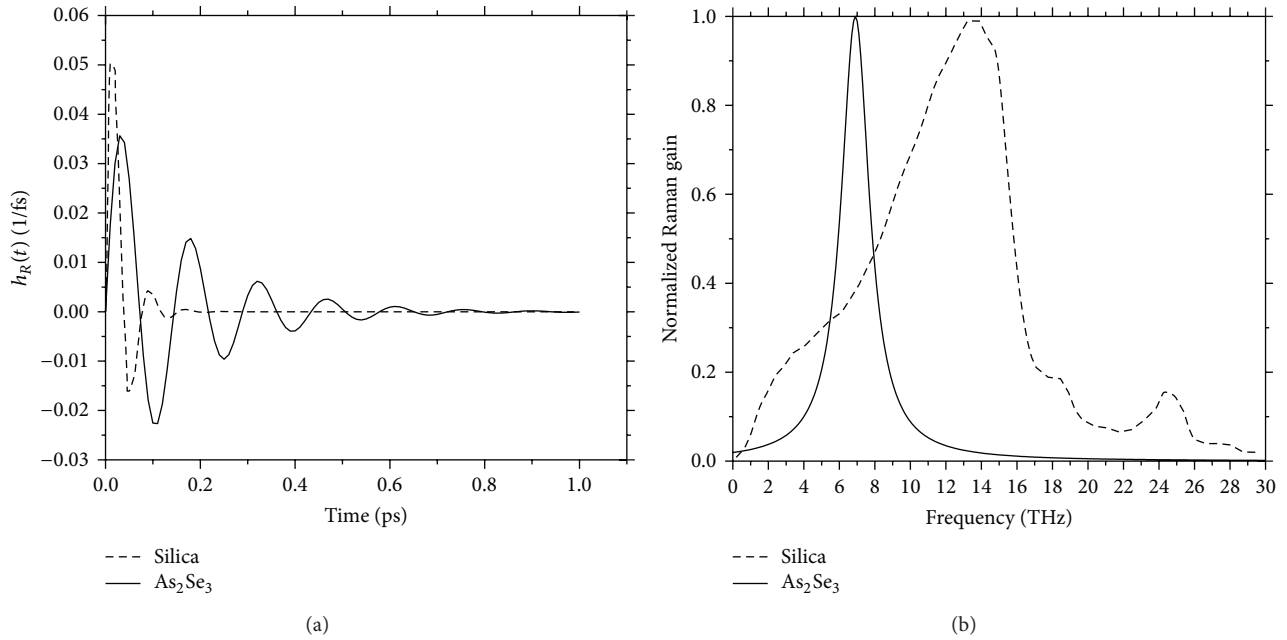

FIGURE 2: (a) Temporal Raman response functions calculated for both As_2Se_3 chalcogenide (solid curve) and silica materials (dashed curve) and (b) the corresponding normalized Raman gains.

the best fit with the results of [10]. The fraction $f_R = (\lambda/2\pi^2 n_2)\int_0^{\infty}(g_R(f)/f)df$ can be calculated from the *Kramers-Kroning* relation and has been found to be equal $f_R = 0.148$ in close agreement with the previously reported values.

3. Study of the Supercontinuum Generation in As_2Se_3-Based PCF

In this section, the generation of supercontinua in the small core highly nonlinear As_2Se_3-based PCFs is investigated. The supercontinuum process is described by the generalized nonlinear Schrodinger equation (GNLSE):

$$\frac{\partial U}{\partial z} = -\frac{\alpha}{2}U - \sum_{m\geq 2}\frac{j^{m-1}\beta_m}{m!}\frac{\partial^m U}{\partial t^m} + j\left(\gamma_0 + i\gamma_1\frac{\partial}{\partial t} - \frac{\gamma_2}{2}\frac{\partial^2}{\partial t^2}\right)\left(1 + \frac{j}{\omega_0}\frac{\partial}{\partial t}\right) \times \left(U(z,t)\int_{-\infty}^{+\infty} R(t')\left|U(z,t-t')\right|^2 dt'\right), \quad (2)$$

where α is the loss coefficient, β_m are the various coefficients in the Taylor series expansion of propagation constant β at the input pulse's central frequency ω_0, and $\gamma(\omega) = n2\omega/cA_{\text{eff}}(\omega)$ is the nonlinear coefficient. The response function $R(t)$ includes the electronic and the vibrational Raman contributions. The GNLSE of (2) is solved numerically using the split-step Fourier method implemented in MATLAB.

In our study, we consider three hole-to-hole spacings of 3.5 μm, 4.5 μm, and 5.5 μm. Compared to the study

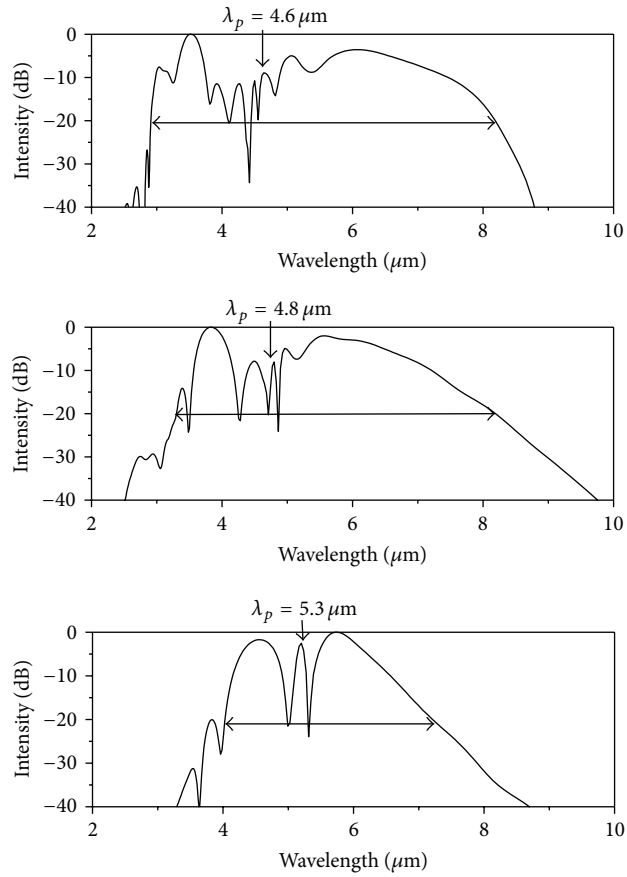

FIGURE 3: Output spectra for $\Lambda = 3.5\,\mu$m (top), 4.5 μm (middle), and 5.5 μm (bottom). The input pulse has a FWHM of 160 fs and a peak power of 1 kW.

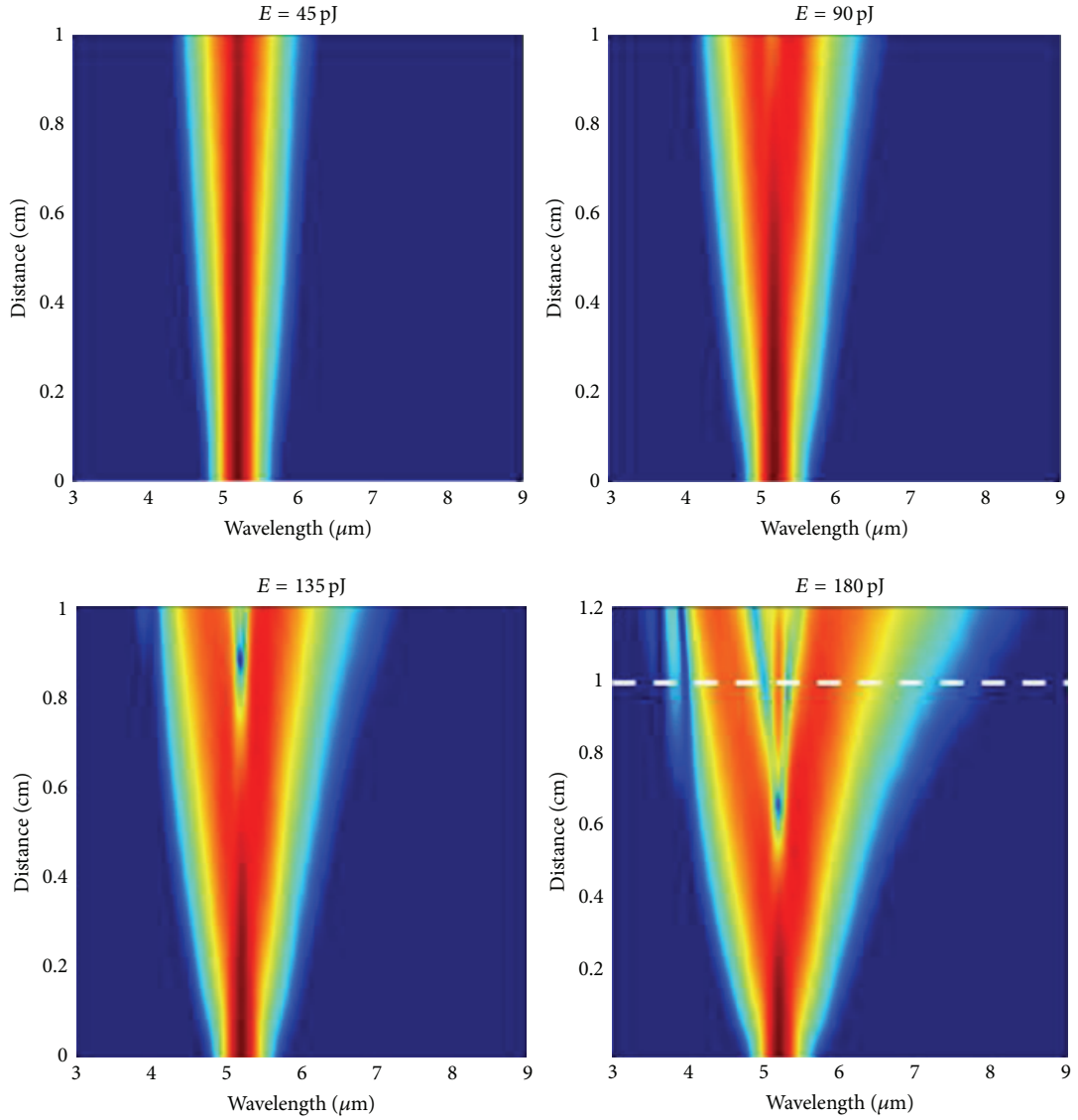

Figure 4: Supercontinua generated in As_2Se_3-based PCF with $d = 2\,\mu$m and $\Lambda = 5\,\mu$m and calculated for different energies of (a) 45 pJ, (b) 90 pJ, (c) 135 pJ, and (d) 180 pJ. The input pulse has a FWHM of 160 fs. – – –Maximum broadening for 1 cm PCF length with 180 pJ input energy (i.e., 1 kW peak power).

performed by Hu et al. in optimizing the bandwidth of the SC generated in As_2Se_3-based PCF, we considered larger PCF structures. Our choice was motivated by considering a bit larger pitch Λ because such structures have more broadening from the soliton self-frequency shift (SSFS) since it is proportional to the dispersion. However, larger structures also lead to an increase in the effective mode area, which decreases modal confinement and hence nonlinearity, which in turn is disadvantageous to the SCG. The choice of the chalcogenide material with high nonlinearity compensates the decrease of the nonlinear coefficient of the PCF structure.

For the simulations, we considered a secant hyperbolic field profile emerging from a tunable femtosecond laser $U(0,T) = \sqrt{P_0}\sec h(T/T_0)$ between $\lambda = 2.5\,\mu$m and $5.5\,\mu$m, where T is the time and T_0 is related to the full width at half maximum (FWHM) pulse duration.

First we focus our study on the SC generation in the anomalous region, where the key factor of the spectral broadening is the solitonic fission. We set a pump wavelength very close to the ZDW to achieve the solitonic fission and remove the effect of four-wave mixing and amplification of higher-order dispersive waves.

Figure 3 shows the output spectra with pitches of $3.5\,\mu$m, $4.5\,\mu$m, and $5.5\,\mu$m. The input pulse has a FWHM of 160 fs with a repetition rate $f = 82$ MHz and a peak power of 1 kW. We define the generated bandwidth as the bandwidth inside frequency limits that are 20 dB down from the peak of the spectrum. For $\Lambda = 5.5\,\mu$m, the total generated bandwidth is more than $3\,\mu$m, as shown in Figure 3. The generated bandwidths were calculated to be around ~$5.3\,\mu$m, $5\,\mu$m, and $3.2\,\mu$m for $\Lambda = 3.5\,\mu$m, $4.4\,\mu$m, and $5.5\,\mu$m, respectively. Thus, the SCG in chalcogenide PCFs is highly influenced by

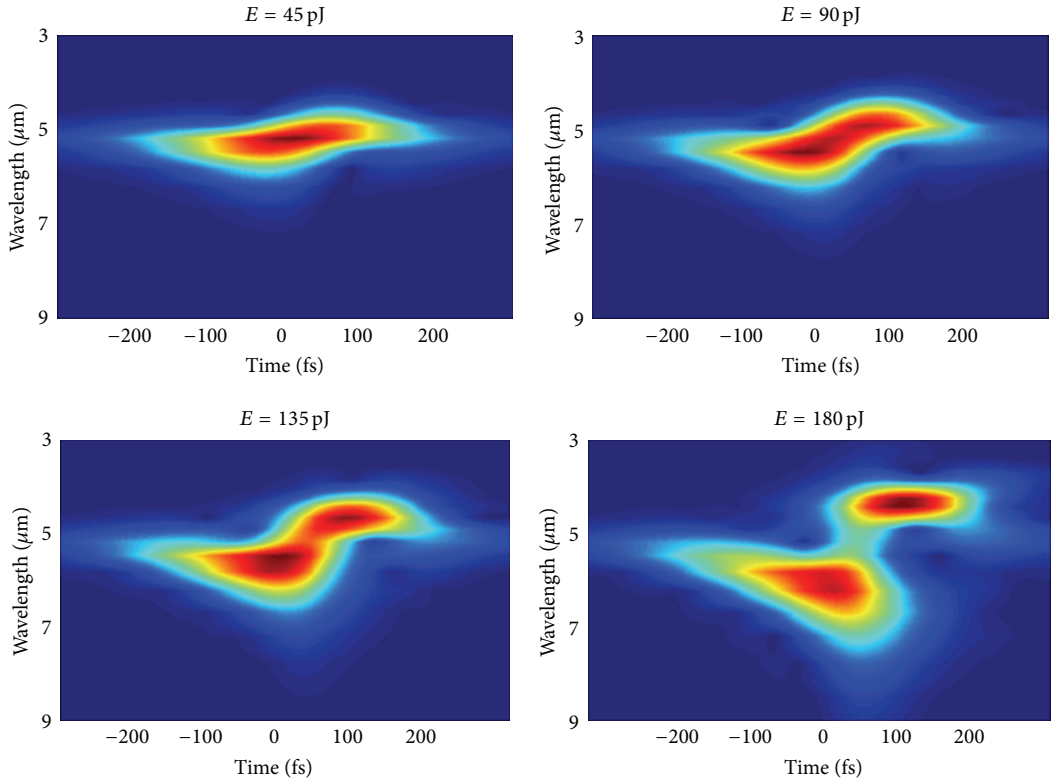

FIGURE 5: Simulated spectrogram representation of the pulse evolution at different energy inside the As_2Se_3-based PCF with projected spectral intensity profile.

the choice of the optogeometrical parameters because they affect the generation of the nonlinear effects. With decreasing the core size of the PCF, the generated bandwidth decreases. So that, a compromise between the core size of the As_2Se_3-based PCF and the generated bandwidth has to be found.

In order to understand the dynamics behind the SCG, we propose to focus on the largest PCF structure since SC was not reported in such a PCF structure. The physical processes leading to the growth of the supercontinuum were studied by increasing the input energy.

Figure 4 shows the supercontinua generated along an As_2Se_3-based PCF when $\Lambda = 5.5\,\mu$m. The generated spectra were calculated for different peak power ranging from 250 to 1000 W corresponding to energies ranging from 45 to 180 pJ. The nonlinear coefficient was calculated to be around $\gamma = 791\,(\text{W}\cdot\text{km})^{-1}$.

As we are pumping close to the ZDW in the anomalous dispersion regime, the mechanisms leading to the SCG are based on the processes of soliton fission and soliton-related dynamics. In the beginning (Figure 4(a)), the effect of self-phase modulation first broadens the spectrum so that it extends into the region around 4.3 μm and 6.3 μm.

When increasing the input power, we observe the growth of a long wavelength peak at $\lambda = 5.4\,\mu$m, which is associated with soliton pulse experiencing the Raman soliton-self frequency shift. We see the generation of the associated dispersive waves responsible for the short wavelength structure in the range of ~4 μm. For the maximum energy coupled into the As_2Se_3-based PCF ($E = 180$ pJ), the SC spectrum covers more than three optical octaves. We clearly observe the threshold, saturation, and stability of the supercontinuum as it approaches the propagation length of 1 cm (as shown by the dashed line in Figure 4(d)) with 180 pJ input energy corresponding to 1 kW peak power. Figure 5 depicts the simulated spectrogram representation of the pulse evolution at different energy inside the As_2Se_3-based PCF with projected spectral intensity profile. We easily confirm from these representations that the effects of self-phase modulation and self-soliton frequency shift due to the Raman effect are predominant and responsible for the broadband generated spectra. The large nonlinearities and fast response of the nonlinearity of the As_2Se_3-based PCF make fibres drawn from this glass well suited for many applications such as spectroscopy, laser induced sources, and optical switches, and optical regenerators for high speed telecommunication systems.

4. Conclusion

We have computationally investigated supercontinuum generation in sub-cm long As_2Se_3-based solid core photonic crystal fiber with a hexagonal cladding of air holes. Ultra-broadband SC was generated in small core chalcogenide PCFs at a peak power of 1 kW. Bandwidths of ~5.3 μm, 5 μm, and 3.2 μm were calculated for $\Lambda = 3.5\,\mu$m, 4.5 μm, and 5.5 μm, respectively. Accurate fit of the Raman response was proposed based on recently published experimental results. The dynamics behind the broadband SC generation in the

mid-IR region is mainly ruled by the SPM and the soliton-self frequency shift due to the Raman effect. These characteristics make SC generated by short and small core As_2Se_3-based PCFs promising for applications requiring fiber based near to mid-IR.

References

[1] J. K. Ranka, R. S. Windeler, and A. J. Stentz, "Visible continuum generation in air-silica microstructure optical fibers with anomalous dispersion at 800 nm," *Optics Letters*, vol. 25, no. 1, pp. 25–27, 2000.

[2] J. M. Dudley and J. R. Taylor, "Ten years of nonlinear optics in photonic crystal fibre," *Nature Photonics*, vol. 3, no. 2, pp. 85–90, 2009.

[3] J. M. Dudley, G. Genty, and S. Coen, "Supercontinuum generation in photonic crystal fiber," *Reviews of Modern Physics*, vol. 78, no. 4, pp. 1135–1184, 2006.

[4] S. Roy and P. R. Chaudhuri, "Supercontinuum generation in visible to mid-infrared region in square-lattice photonic crystal fiber made from highly nonlinear glasses," *Optics Communications*, vol. 282, no. 17, pp. 3448–3455, 2009.

[5] R. J. Weiblen, A. Docherty, J. Hu, and C. R. Menyuk, "Calculation of the expected bandwidth for a mid-infrared supercontinuum source based on As_2S_3 chalcogenide photonic crystal fibers," *Optics Express*, vol. 18, no. 25, pp. 26666–26674, 2010.

[6] A. B. Fedotov, A. M. Zheltikov, A. A. Ivanov et al., "Supercontinuum-generating holey fibers as new broadband sources for spectroscopic applications," *Laser Physics*, vol. 10, no. 3, pp. 723–726, 2000.

[7] J. H. V. Price, T. M. Monro, H. Ebendorff-Heidepriem et al., "Mid-IR supercontinuum generation from nonsilica microstructured optical fibers," *IEEE Journal on Selected Topics in Quantum Electronics*, vol. 13, no. 3, pp. 738–749, 2007.

[8] P. Domachuk, N. A. Wolchover, M. Cronin-Golomb et al., "Over 4000 nm bandwidth of Mid-IR supercontinuum generation in sub-centimeter segments of highly nonlinear tellurite PCFs," *Optics Express*, vol. 16, no. 10, pp. 7161–7168, 2008.

[9] L. B. Shaw, V. Q. Nguyen, J. S. Sanghera, I. D. Aggarwal, P. A. Thielen, and F. H. Kung, "IR supercontinuum generation in As-Se photonic crystal fiber," in *Proceedings of the Advanced Solid-State Photonics (ASSP '05)*, paper TuC5, pp. 864–868, Vienna, Austria, February 2005.

[10] J. Hu, C. R. Menyuk, L. B. Shaw, J. S. Sanghera, and I. D. Aggarwal, "Maximizing the bandwidth of supercontinuum generation in As_2Se_3 chalcogenide fibers," *Optics Express*, vol. 18, no. 7, pp. 6722–6739, 2010.

[11] J. A. Savage, "Optical properties of chalcogenide glasses," *Journal of Non-Crystalline Solids*, vol. 47, no. 1, pp. 101–116, 1982.

[12] G. Boudebs, S. Cherukulappurath, M. Guignard, J. Troles, F. Smektala, and F. Sanchez, "Linear optical characterization of chalcogenide glasses," *Optics Communications*, vol. 230, no. 4–6, pp. 331–336, 2004.

[13] R. Cherif, A. B. Salem, M. Zghal et al., "Highly nonlinear As_2Se_3-based chalcogenide photonic crystal fiber for midinfrared supercontinuum generation," *Optical Engineering*, vol. 49, no. 9, Article ID 095002, 6 pages, 2010.

[14] R. Cherif, M. Zghal, I. Nikolov, and M. Danailov, "High energy femtosecond supercontinuum light generation in large mode area photonic crystal fiber," *Optics Communications*, vol. 283, no. 21, pp. 4378–4382, 2010.

[15] M. Zghal and R. Cherif, "Impact of small geometrical imperfections on chromatic dispersion and birefringence in photonic crystal fibers," *Optical Engineering*, vol. 46, no. 12, Article ID 128002, 7 pages, 2007.